

COLD FUSION PHENOMENON AND ITS APPLICATION TO ENERGY PRODUCTION AND NUCLEAR WASTE REMEDIATION

H. Kozima
Portland State University

ABSTRACT

The Cold Fusion Phenomenon (CFP) is concerned with nuclear reactions and accompanying events occurring in solids with high densities of hydrogen isotopes in ambient radiation. It is now recognized as a rather widespread phenomenon, including various nuclear transmutations in the surface or boundary layers of transition-metal hydrides and deuterides. Characteristics of the CFP are deduced from experimental data sets showing qualitative reproducibility, sporadic and intermittent occurrence, localized reactions in surface layers, a variety of elements produced by nuclear transmutation (NT), and definite quantitative relations between the amounts of these products. A unified and systematic explanation of experimental data sets in the CFP has been developed in the framework of modern physics, based on a model (TNCF model) assuming the existence of quasi-stable thermal neutrons in solids. (quantum mechanical verification of the premises assumed in the model is given, using knowledge of solid state physics and nuclear physics. It shows that there is a big difference of nuclear reactions in free space and in CF materials when there exist neutron Bloch waves. The physics of CFP allows us to contemplate its application to various processes that produce nuclear transmutations and excess energy.

INTRODUCTION

The discovery of the cold fusion phenomenon (CFP) in 1989 by M. Fleischmann et al. [1] and S.E. Jones et al. [2] in experiments assumed the occurrence of d-d fusion reactions in transition-metal deuterides. The quantum mechanical evaluations of the reaction rates of the d-d fusion reactions in solids [3,4] denied the reality of its observation as results of anticipated reactions. Although there have been several kinds of trials to facilitate d-d fusion reactions in solids, the negative conclusion [3,4] seems not overturned. To explain various experimental results obtained in these more than 12 years, the present author proposed a model [5] based on characteristics of experimental data on CFP assuming neutrons in CF materials free from the Coulomb barrier problem and successfully explained whole experimental data sets on CFP. In this paper, we give a summary of the experimental results, essential concepts of the TNCF model, consistent explanation of experimental data sets by the model, quantum mechanical verification of the model, and possible applications of CFP.

EXPERIMENTAL DATA SETS OF CFP

Experimental results related to the cold fusion phenomenon (CFP) are classified into the following events: excess energy (Q), nuclear transmutations (NT), production of helium-4 (${}^4_2\text{He}$) and tritium (${}^3_1\text{H} = \text{T}$), emissions of neutrons (n), gammas (γ), X-rays (X), alphas (α), and protons (p). The nuclear transmutations are divided into three types, NT_D , NT_F , and NT_A , in relation with pre-existing nuclides ${}^A_Z\text{M}$'s in the experimental system. The nuclear products by NT in CFP are explained as (1) decay products of a nuclide ${}^{A+v}_Z\text{M}$ formed from ${}^A_Z\text{M}$ by absorption of v neutrons (NTD) with the decay-time shortening, (2) fission products of a nuclide ${}^{A+v}_{Z+p}\text{M}'$ formed by absorption of a neutron-proton cluster ($v\eta, \rho\rho$) (NT_F) with the fission-barrier lowering, and (3) stable nuclides ${}^A_{Z'}\text{M}'$ formed from ${}^A_Z\text{M}$ by absorption of a cluster ($v\eta, \rho\rho$) ($v = A' - A, \rho = Z' - Z$) (NT_A).

These events are also classified into direct and indirect evidence for nuclear reactions in solids, as tabulated in Table 1 [5], with some characteristics of experimental data sets. In Table 1, "Agents" express necessary elements to be added to the matrix substances without direct correlation in the order in the column except neutron (n), which seems necessary for all experiments where positive results occurred. These events of CFP have several characteristics deduced from experimental data sets: qualitative reproducibility; sporadic and intermittent occurrence; localized reactions; optimum combinations of transition metal – [hydrogen isotopes – [electrolyte]; and variety of nuclides produced by nuclear transmutation (NT). Several necessary conditions for those events in CFP confirmed by now are listed as follows:

1. existence of hydrogen isotopes (protium and/or deuterium) in appropriate solids (Pd, Ti, Ni, and so forth),
2. existence of the background thermal neutrons,
3. existence of an appropriate alkali-metal layer (Li, K, Na and so forth) on the surface of the metal hydride (in the case of electrolytic system with alkaline metal), and
4. inhomogeneous distribution of hydrogen isotope in the solid suggested by nonequilibrium conditions in experiments.

It should be emphasized that sufficient conditions of the cold fusion phenomenon are not determined yet although these necessary conditions have been recognized in the experimental data sets obtained hitherto.

TABLE 1. MATRIX SUBSTANCES, AGENT NUCLEI, DIRECT AND INDIRECT EVIDENCE OF NUCLEAR REACTIONS IN COLD FUSION PHENOMENON (CFP). Q is for the excess heat and NT for the nuclear transmutation); energy ϵ and position r dependences of products, decay time shortening of radioactive nuclides, and fission- barrier lowering of compound nuclides give direct information of nuclear reactions in CFP.

Matrix Substance	Agent	Direct Evidence	Indirect Evidence
Pd, Ti, Ni	${}^2_1\text{H} \equiv d$	Gamma rays γ (ϵ)	Excess heat Q
KCl + LOCl	${}^1_1\text{H} \equiv p$	Neutron energy spectra n (ϵ)	Neutrons n
ReBa ₂ Cu ₃ O ₇	${}^6_3\text{Li}$	Spatial distribution	Tritium ${}^3_1\text{H}$ - T
Na _x W ₀₃	${}^{10}_5\text{B}$	of NT products (${}^A_Z M(r)$)	Helium ${}^4_2\text{He}$
KD ₂ PO ₄	${}^{39}_{19}\text{K}$	Decay time shortenings	NT (NT _D , NT _F , and NT _A)
TGS	${}^{85}_{37}\text{Rb}$, ${}^{87}_{37}\text{Rb}$	Fission-barrier lowering	X-ray X(ϵ)
SrCe _a Y _b Nb _c O _d	${}^1_0n \equiv n$		

There are definite relations between amounts N_X of a product X . The relations for these products N_Q , N_{NT} , N_{He4} , N_T , N_n , and N_γ are expressed as follows;

$$N_Q \sim N_{NT} \sim N_{He4} \sim N_T \sim 107 N_n, N_\gamma \sim 0 \quad (1)$$

Lack of γ -ray emissions, which usually accompany nuclear reactions in free space, is one of riddles of nuclear reactions in CFP.

TRAPPED NEUTRON CATALYZED FUSION (TNCF) MODEL FOR CFP

The TNCF model [5,6] is a phenomenological model with a single adjustable parameter n_n . To interpret various experimental data sets with qualitative reproducibility (or irreproducibility) and their absence in environment without background neutrons, the author constructed a model, named later the "TNCF model." The TNCF model has numerous premises based on the experimental data, as explained herein. These fundamental premises symbolize several necessary conditions of the cold fusion phenomenon, extracted from these data by the author. The TNCF model has been applied to analyze more than 60 data sets obtained in various circumstances and materials; the results have been published one by one in Ref. [5] and compiled and published in Ref. [6].

In the model, there is one adjustable parameter n , the density of the trapped thermal neutrons, which is used to analyze the cold fusion phenomenon containing several events specified by some physical quantities supposed to be results of various physical processes in the material. Some examples of these physical quantities are (1) distribution of transmuted nuclei in the material, neutron energy spectra, and gamma ray spectra, and (2) the excess heat, amounts of generated tritium and helium in a definite time, and X-ray and other charged particles if any. The quantities in Group 1 are direct information of nuclear reactions in CF materials and those in Group 2 are indirect information as accumulated results of the reactions.

Thus, it is possible to interpret various, sometimes more than two events in the cold fusion phenomenon consistently assuming only one adjustable parameter n_n with a reservation of inexplicable problem of poor reproducibility and lack of simultaneity of several events. To understand these unexplained points more clearly, it will be necessary to take details of the object materials into the analyses on the TNCF model.

PREMISES OF THE TNCF MODEL

In this subsection, we will explain fundamental concepts of the TNCF model and relevant reactions in detail. The TNCF model is a phenomenological one. The basic premises (assumptions) extracted from experimental data sets [5,6] are summarized as follows:

Premise 1. We assume a priori existence of the quasi-stable, trapped neutron with a density n_n in pertinent solids, to which the neutron is supplied essentially from the ambient neutron at first and then by breeding processes (explained below) in the sample. The density n_n is an adjustable parameter in the TNCF model that will be determined by an experimental data set using the supplementary premises, which will be explained below concerning reactions of the trapped neutron with other particles in the solids. The quasi-stability of the trapped neutron means

that the neutron trapped in the crystal does not decay until a strong perturbation destroys the stability while a free neutron decays with a time constant of 887.4 ± 0.7 s.

Premise 2. The trapped neutron in a solid reacts with another nucleus in the surface layer of the solid, where it suffers a strong perturbation, as if they are in vacuum. We express this property by taking the parameter (the instability parameter) ξ , defined in the relation (2) written down below, as $\xi = 1$. We have to mention here that the instability parameter ξ in the surface layer is not known at all and it can be, as noticed recently, more than one ($1 \leq \xi$) making the determined value of the parameter n , smaller. This ambiguity is suggested by various anomalous changes of decay character of radioactive isotopes and by unexpected fission products in the surface layer.

Premise 3. The trapped neutron reacts with another perturbing nucleus in volume by a reaction rate given in the relation (2) below with a value of the instability parameter $\xi \leq 0.01$ due to its stability in the volume (except in special situations such as at very high temperature as 3000 K). Other premises closely related with numerical calculations of n_n from experimental data are common to all data analyses and are not described here. (Cf. Refs. [5,6] for details of these premises of the TNCF model.)

If the stability of the trapped neutron is lost by a large perturbation in the surface layer or in volume, the number N of trigger reactions (per unit time) between trapped thermal neutrons and a nucleus ${}_Z^A M$ may be calculated by the same formula as the usual collision process in vacuum but an instability parameter ξ :

$$N = 0.35 n_n v_n n_m V \sigma_{mM} \xi \quad (2)$$

where $0.35 n_n v_n$ is the flow density of the trapped thermal neutron per unit area and time, n_m is the density of the nucleus, V is the volume where the reaction occurs, σ_{mM} is the cross section of the reaction. The instability parameter ξ as taken into the relation (2) expresses an order of the stability of the trapped neutron in the region as explained in Premises 2 and 3.

In the electrolytic experiments, we have taken $\xi = 1$ in the surface layer and $\xi = 0$ in the volume except otherwise stated (Premises 2 and 3). The values of $\xi = 0.01$ instead of $\xi = 0$ in the relation (2) will result in lower n , in the electrolytic data by a factor 2 than that determined with a value $\xi = 0$ as had been used in our former analyses. (In this section, we will cite previous results with $\xi = 0$ as they were.)

If a fusion reaction occurs between a trapped thermal neutron and one of lattice nuclei ${}_Z^A M$ with a nucleon number A and a proton number Z , there appears an excess energy Q and nuclear products as follows:

$$n + {}_Z^A M = {}_{Z-a}^{A+1-b} M' + {}_a^b M'' + Q$$

where ${}_0^1 M \equiv \gamma$, ${}_1^1 M \equiv n$, ${}_1^2 M \equiv d$, ${}_2^3 M \equiv t$, ${}_2^4 M \equiv {}^4\text{He}$, etc.

The liberated energy Q may be measured as the excess heat by the attenuation of the energy of nuclear products, γ or charged particles, as generated in the n - d reaction. Otherwise, the nuclear products may be observed outside with energies (we assume it as the original one, hereafter) or may induce succeeding nuclear reactions (cf. "Breeding Reactions") with one of other nuclei in the sample.

NUCLEAR REACTIONS RELEVANT TO THE TNCF MODEL

Typical reactions relevant with TNCF model had been written down as follows with supplementary explanations.

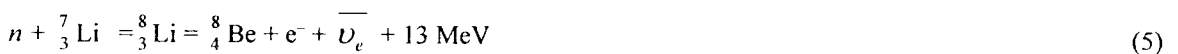
Trigger Reactions. The trapped thermal neutron can fuse with ${}_3^6\text{Li}$ nucleus by the following reaction in the surface layer formed on the cathode by electrolysis of D_2O (H_2O) + LiOD (LiOH) with a large cross section $\sim 1 \times 10^3$ b ($1 \text{ b} = 10^{-24} \text{ cm}^2$) (at 300 K):



The thickness of the surface layer will be assumed as $1 \mu\text{m}$ throughout the following analysis although it has been determined as $1\sim 10 \mu\text{m}$ in experiments (allowing one order of magnitude uncertainty in the determined value of n_n).

Also, the abundance of the isotope ${}_3^6\text{Li}$ will be assumed as the natural one, i.e., 7.4% except otherwise described.

A trapped thermal neutron can fuse effectively with a deuteron by the following reaction (4) in volume and with ${}_3^7\text{Li}$ nucleus by the reaction (5) in the surface layer, respectively:



$$\frac{8}{4} \text{Be} = 2 \frac{4}{2} \text{He} + 3.2 \text{ MeV} \quad (6)$$

The reaction (4) for a thermal neutron has a cross section 5.5×10^{-4} b and the reaction (5) has 4×10^{-2} b, which will be used in the calculation given in the following sections.

In the case of solids with protium but deuterium, the following reaction should be taken up in the analysis as the trigger reaction:

$$n + p = d (1.33 \text{ keV}) + \gamma (2.22 \text{ MeV}). \quad (7)$$

The fusion cross section of the reaction (7) for a thermal neutron is 3.5×10^{-1} b, which is fairly large compared with that of the reaction (4).

Breeding Reactions. The triton with an energy $\varepsilon = 2.7$ MeV (or 6.98 keV) generated in the reaction (3) (or (4)) can pass through the crystal along the channeling axis on which is an array of occluded deuterons or can proceed a finite distance with a path length $\ell_t (\cong 1 \sim 10 \mu\text{m})$ determined by the interaction with charged particles in the crystal. In the process of penetration through a crystal, the triton can react with a deuteron by the following reaction on the path with a length 1 μm :

$$t + d = \frac{4}{2} \text{He} (3.5 \text{ MeV}) + n (14.1 \text{ MeV}). \quad (8)$$

The cross section of this reaction is $\sigma_{t-d} \sim 1.4 \times 10^{-1}$ b for $\varepsilon = 2.7$ MeV and 3.04×10^{-6} b for 6.98 keV.

It has been a defect in experimental researches not trying to detect higher energy neutrons up to 15 MeV expected to be generated in this reaction (8). In the following analysis, we assume the path length of 2.7 MeV triton as $\ell_t = 1 \mu\text{m}$ throughout this paper.

The neutron with 14.1 MeV generated in the reaction (8) can interact with particles in the crystal, especially with a deuteron elastically giving a large amount of energy to it or inelastically dissociating it:

$$n + d = n' + d' \quad (9)$$

$$n + d = n' + p + n'' \quad (10)$$

$$n + \frac{A}{Z} \text{M} = \frac{A}{Z} \text{M} + n' \quad (11)$$

$$n + \frac{A}{Z} \text{M} = \frac{A-A'+1}{Z-Z'} \text{M}' + \frac{A'}{Z'} \text{M}'' \quad (12)$$

In these reactions, the high-energy neutron loses its energy to be thermalized or generate another low energy neutron to be trapped in the sample (breeding processes) or generate transmuted nuclei. The deuteron having an energy up to 12.5 MeV accelerated elastically in the scattering (9) by the neutron with 14.1 MeV can fuse with another deuteron in two modes by the following reactions with a fairly large cross section of the order of 0.1 b each:

$$d + d = t (1.01 \text{ MeV}) + p (3.02 \text{ MeV}) \quad (13)$$

$$= \frac{3}{2} \text{He} (0.82 \text{ MeV}) + n (2.45 \text{ MeV}) \quad (14)$$

Branching ratios of these reactions are, as is well known, 1 : 1. Another possibility is the reaction with small relative probability 10^{-7} compared with the above two:

$$d + d = \frac{4}{2} \text{He} (76.0 \text{ keV}) + \gamma (23.8 \text{ MeV}). \quad (15)$$

To analyze experimental data in electrolytic systems, we have taken an abundance of $\frac{6}{3}\text{Li}$ in LiOD as the natural one 7.42%, an average velocity of the trapped neutron $v_n = 2.2 \times 10^5$ cm/s ($kT \sim 1/40$ eV at $T = 300$ K). Then, we can determine the density of the trapped neutron n_n using the above relation (1) between n_n and the number of tritium atom N_t (= number of helium atom N_{He}) generated in the surface layer in a time τ ,

$$N_t = N_{He} = 0.35 n_n v_n n_{dLi} \ell S \sigma_n \tau \xi \quad (16)$$

where S is a surface area of the cathode, ℓ is the thickness of the Li surface layer, $\sigma_{nLi} = 10^3$ b, $n_{dLi} = 3.5 \times 10^{21}$ cm $^{-3}$ and ξ is the instability parameter (which we take as 1 in the surface layer).

In general, the number of events (reactions) N_{nM} in time τ between the trapped neutron and the lattice nuclei $\frac{A}{Z} \text{M}$ in a volume V of a sample is given by similar relation:

$$N_{nM} = 0.35 n_n v_n n_M V \sigma_{nM} \tau \xi \quad (17)$$

where n_M is the density of the nucleus M , σ_{nM} is the cross section of the reaction and ξ is the instability parameter (which we take as 0.01 in volume using experimental data).

The number of tritium atom determined by the relation (16) is also number of events N_Q generating the excess heat of 4.8 MeV per a reaction:

$$N_t = N_Q \equiv Q \text{ (MeV)} / 4.8 \text{ (MeV)} \quad (18)$$

This relation is in accordance with experimental data shown in Tables 2-5 and in the relation (1) by a factor about 3.

A relation between N_n and N_t in D/Li system is given as follows; when the $n - {}^6_3\text{Li}$ reaction (3) is predominant over the reaction (4) in an electrolytic system with D_2O , neutron is generated by the reaction (8) giving a relation between N_n and N_t assuming half of the generated triton in (3) contribute the reaction (8),

$$N_n - N_t \ell_t n_d \sigma_{t-d} \quad (19)$$

where $\ell_t \sim 1 \mu\text{m}$, $n_d = 6.8 \times 10^{22} \text{ cm}^{-3}$ ($x = \text{D/Pd}$ ratio in the sample) and $\sigma_{t-d} \sim 1.4 \times 10^{-1} \text{ b}$. For $x = 1$, we obtain a relation

$$N_n/N_t = 9.5 \times 10^{-7}, 10^{-6} \quad (20)$$

This relation is in accordance with experimental data shown in Tables 2-5 and in the relation (1) by a factor about 3.

Neutron Drop-Nucleus Reactions. As explained below ("Quantum Mechanical ..."), there is a possibility of forming neutron drops (clusters of large number of neutrons and a few protons) in boundary layers. Let us use a symbol ${}^A_Z \Delta$ for a neutron drop with $(A - Z)$ neutrons and Z protons where $A \gg Z$. Then, the interaction of a nucleus ${}^A_Z \text{M}$ and a neutron drop ${}^{A'}_{Z'} \Delta$ results in formation of a new nuclide ${}^{A''}_{Z''} \text{M}'$ with $A'' \gg A, Z'' \gg Z$:



where $A + A' = A'' + A'''$, $Z + Z' = Z'' + Z'''$ should be satisfied. The neutron drop ${}^{A'''}_{Z'''} \Delta$ is turned into ${}^{A'}_{Z'} \Delta$ through the interaction with a thin neutron gas in the background. The new nuclide ${}^{A''}_{Z''} \text{M}'^*$ stabilizes (1) by fission (fission-barrier lowering) or decay (decay-time shortening) generating several new nuclides, or (2) by losing energy to be a stable nuclides ${}^{A''}_{Z''} \text{M}'$. In these processes occurring in contact with a thin neutron gas, there are many branches to dissipate energies of excited states, which should be liberated only through a γ -ray emission in free space. This is a fundamental difference of nuclear reactions in CF materials from those in the free space and may be the reason of the lack of γ -rays in UP, an unsolved riddle until now.

EXPLANATION OF EXPERIMENTAL DATA SETS BY THE TNCF MODEL

The premises [5] in the TNCF model, explained briefly in "Premises of the TNCF Model," connect n_n and the observed quantities (not necessarily simultaneously). With these premises, more than sixty typical experimental data sets including those by Fleischmann et al. [1], and others were analyzed [1,2] successfully with consistency in them [5,6]. The main results of these analyses on the more than 60 data sets are tabulated in Tables 2-5. The parameter n_n was determined from the data sets in experiments as $10^8 \sim 10^{10} \text{ cm}^{-3}$.

One of the most remarkable results obtained in the analyses by the TNCF model is a possibility of explaining several events (e.g., Q and NT) with only one adjustable parameter n_n . Typical cases are data of Nos. 1, 4, 8, 9, 14, 19, 36, and 37 in the Tables 2-5 where theoretical ratios of numbers of events $N_x/N_{x'}$ (in "Other Results") coincide with experimental ones (in "Measured Quantities") within a factors of about 3. The difficulty to explain production of ${}^4_2\text{He}$ in the electrolytic system of Pd/ D/Li were resolved by the reaction between the trapped neutron and ${}^6_3\text{Li}$ occurring in the surface layer of Li metal (and/or PdLi_x alloy) on the cathode.

QUANTUM MECHANICAL VERIFICATION OF PREMISES OF THE TNCF MODEL

A unified and systematic explanation of experimental data sets in the CFP based on the TNCF model given in the preceding subsection should be investigated using quantum mechanics on the basis of solid state physics and nuclear physics. In this subsection we give a quantum mechanical verification of the premises assumed in the TNCF model. Key elements of the explanation are neutron bands in solids and neutron drops made of large number of neutrons and a few protons and electrons in surface layers.

TABLE 2. RESULTS OF TNCF MODEL ANALYSES, SEE "EXPLANATION OF EXPERIMENTAL DATA..."
(1) Pd/D(H)/Li System. Neutron density n_n and relations between the numbers N_x of event x obtained by theoretical analysis of experimental data on TNCF model ($N_Q \equiv Q \text{ (MeV)}/5 \text{ (MeV)}$). Typical value of the surface vs. volume ratio $S/V(\text{cm}^{-1})$ of the sample is tabulated also. Refs.in this table are those in Ref. [5].

Data No.	Authors	System	S/V cm^{-1}	Measured Quantities	n_n cm^{-3}	Other Results (remarks)
1	Fleischmann et al. [1]	Pd/D/Li	6 ~ 40	Q, t, n $N_t/N_n \sim 4 \times 10^7$ $N_Q/N_t \sim 0.25$	$\sim 10^9$	$(Q = 10\text{W}/\text{cm}^3)$ $N_t/N_n \sim 10^6$ $N_Q/N_t = 1.0$
2	Morrey et al. [1-4]	Pd/D/Li	20	$Q, {}^4\text{He}$ ${}^4\text{He}$ in $\ell \leq 25 \mu\text{m}$	4.8×10^8	$N_Q/N_{He} \sim 5.4$ (If 3% ${}^4\text{He}$ in Pd)
3	Packham [43]	Pd/D/Li	40	t in solution	3.6×10^7	
4	Chien et al. [43]	Pd/D/Li	4	${}^4\text{He}$ in surf. layer and t , no ${}^3\text{He}$	1.8×10^{12}	$N_t/N_{He} \sim 1$ (If few % ${}^4\text{He}$ in Pd)
5	Roulette [1'']	Pd/D/Li	63	Q	$\sim 10^{12}$	
6	Storms [4]	Pd/D/Li	9	$i(1.8 \times 10^2 \text{ Bq/ml})$	2.2×10^7	$(\tau = 250\text{h})$
7	Storms [4']	Pd/D/Li	22	$Q (Q_{\max} = 7\text{W})$	5.5×10^{10}	$(\tau = 120\text{h})$
8	Takahashi et al. [5]	Pd/D/Li	2.7	$t, n N_t/N_n \sim 6.7 \times 10^4$	3×10^5	$N_t/N_n \sim 5.3 \times 10^5$
9	Miles et al. [18']	Pd/D/Li	5	$Q, {}^4\text{He} (N_Q/N_{He} = 1-10)$	$\sim 10^{10}$	$N_Q/N_{He} \sim 5$
10	Okamoto et al. [12']	Pd/D/Li	23	$Q, NT_D \ell_0 \sim 1 \mu\text{m}$	$\sim 10^{10}$	$N_Q/N_{NT} \sim 1.4$ (${}^{27}\text{Al} \rightarrow {}^{28}\text{Si}$)
11	Oya [12-5]	Pd/D/Li	41	Q, γ spectrum	3.0×10^9	(with ${}^{242}\text{Cf}$)
12	Arata et al. [14]	Pd/D/Li	7.5 $\times 10^4$	$Q, {}^4\text{He} (10^{20} \sim 10^{21} \text{ cm}^{-3})$ $N_Q/N_{He} \sim 6$	$\sim 10^{12}$	(Assume t channeling in Pd wall)
13	McKubre [3]	Pd/D/Li	125	Q (& Formula)	$\sim 10^{10}$	Qualit. explan.
14	Passell [3'']	Pd/D/Li	400	NT_D	1.1×10^9	$N_{NT}/N_Q = 2$

TABLE 3. RESULTS OF TNCF MODEL ANALYSES, SEE "EXPLANATION OF EXPERIMENTAL DATA...". (1) Pd/D(H)/Li System (continued from Table 2).

Data No.	Authors	System	S/V cm^{-1}	Measured Quantities	N_n cm^{-3}	Other Results (remarks)
15	Cravens [24'']	Pd/H/Li	4000	$Q (Q_{\text{out}}/Q_{\text{in}} = 3.8)$	8.5×10	(If PdD exists)
16	Bockris [43]	Pd/D/Li	5.3	$t, {}^4\text{He}; N_t/N_{He} \sim 240$	3.2×10	$N_t/N_{He} \sim 8$
17	Lipson [15-4]	Pd/D/Na	200	$y (E\gamma = 6.25 \text{ MeV})$	4×167	If eff. = 1%
18	Will [45]	Pd/DZSOn	21	$i(1.8 \times 10^5 \text{ cm}^2\text{s})$	3.5×10^7	(If $\ell_0 \sim 10 \mu\text{m}$)
19	Cellucci et al. [51'']	Pd/D/Li	40	$Q, {}^4\text{He}$ $N_Q/N_{He} = 1 \sim 5$	2.2×10^9	(If $Q = 5 \text{ W}$) $N_Q/N_{He} = 1$
20	Celani [32'']	Pd/D/Li	400	$Q (Q_{\max} = 7 \text{ W})$	1.0×10^{12}	(If 200% output)
21	Ota [53]	Pd/D/Li	10	$Q (113\%)$	3.5×10^{10}	$(\tau = 220 \text{ h})$
22	Gozzi [51']	Pd/D/Li	14	$Q, t, {}^4\text{He}$	$\sim 10^{11}$	$(\tau \sim 10^3 \text{ h})$
23	Bush [27']	Ag/PdD/Li	2000	$Q (Q_{\max} = 6 \text{ W})$	1.1×10^9	$(\tau = 54\text{d, Film})$
24	Mizuno [26-4]	Pd/D/Li (If Cr in Pd)	3.4	$Q, NT_D \ell \leq 2 \mu\text{m}$	2.6×10^8	$\tau = 30\text{d, Pd}$ $1 \text{ cm}\phi \times 10 \text{ cm}$
25	Iwamura [17]	PdD _x	20	$n (400/\text{s}), t$	3.9×10^8	$4.4 \times 10^6 t/\text{s}$
26	Itoh [17']	PdD _x	13.3	$n (22/\text{s}), t$	8.7×10^7	$7.3 \times 10^{10} t/\text{s}$
27	Itoh [17'']	PdD _x	13.3	$n (2.1 \times 10^3/\text{s})$	3.9×10^8	
28	Iwamura [17'']	PdD _x	20	$Q (4 \text{ W})$ $NT_F(\text{Ti, Cr, etc.})$	3.3×10^{10}	($NT_F?$) unexplained
29	Miley [65]	Pd/H/Li	150	$NT_F(\text{Ni, Zn, ...})$	4.5×10^{12}	
30	Dash [59]	Pd/D, H ₂ SO ₄	57	Q, NT_D	$\sim 10^{12}$	Pt \rightarrow Au
31	Szpak et al. [79-9]	Pd/D/Li	$10^3 (?)$	t	$\sim 10^2$	Electroplated Pd
32	Clarke et al. [80]	Pd/D/Li	$0.26 (?)$	$(Q), t$	$\sim 10^{10}$	Pd black [14]
33	Kozima [203]	Pd/D, H/Li	200	$n (2.5 \times 10^{-4}/\text{s})$	2.5×10^2	Eff. = 0.44%

TABLE 4. RESULTS OF TNCF MODEL ANALYSES, SEE "EXPLANATION OF EXPERIMENTAL DATA...".
(2) Ni/H/K System and others. Explanation of this table is common to Table 2.

Data No.	Authors	System	S / V cm ⁻¹	Measured Quantities	n_p cm ⁻³	Other Results (remarks)
34	Jones [2]	Ti/D/Li	8.1	n (2.45 MeV)	3.1×10^{11}	
35	Mills [25]	Ni/H/K	160	Q (0.13 W)	3.4×10^{10}	
36	Bush [27]	Ni/H/K Ni/H/Na	- 160 - 160	NT_D (Ca) NT_D (Mg)	5.3×10^{10} 5.3×10^{11}	$N_Q/N_{NT} \sim 3.5$ if $\tau = 0$ for ^{40}K
37	Bush [27"]	Ni/H/Rb	- 10	NT_D (Sr)	1.6×10^7	$N_Q/N_{NT} \sim 3$
38	Savvatimova et al. [34"]	Pd/D ₂	100	NT_D (Ag)	9×10^{10}	
39	Bockris et al. [43-6]	Pd/H/		NT_F (Mg, Si, Cs, Fe, etc., in 11 μm layer)	3.0×10^{11}	Only Fe (10% of Pd) is taken up.
40	Alekseev[44]	Mo/D ₂	4.1	t ($\sim 10^7/\text{s}$)	1.8×10^7	(If MoD)
41	Romodanov et al. [44"]	TiC/D	4.1	t ($\sim 10^6/\text{s}$)	$\sim 10^6$	(D/Ti \sim 0.5 assumed)
42	Reifensch- Weiler [38']	TiT _{0.0035}	7×10^9	β decay reduction	1.1×10^9	(T=0 \sim 450 °C)
43	Dufour [7]	Pd, SS/D ₂ Pd, SS/H ₂	48	Q, t, n	9.2×10^{11} 4.0×10^9	(D(H)/Pd \sim 1 is assumed)
44	Claytor [9]	Pd/D ₂	400	t (12.5 nCi/h)	1.6×10^{13}	(If D/Pd \sim 0.5)
~ 45	Srinivasan [16]	Ti/D ₂	1500	t ($t/d \sim 10^{-5}$)	1.9×10^8	(Aged plate)
46	De Ninno [6]	Ti/D ₂	440	n, t	1.2×10^6	(D/Ti=1,lw)

TABLE 5. RESULTS OF TNCF MODEL ANALYSES, SEE "EXPLANATION OF EXPERIMENTAL DATA...".
(2) Ni/H/K System and others (continued). $\Delta(x)$ in this table means a change in the quantity x in the experiment.

Data No.	Authors	System	S / V cm ⁻¹	Measured Quantities	n , cm ⁻³	Other Results (remarks)
47	Focardi [23]	Ni/HZ	8.2	Q	3.0×10^{12}	(If $N_P=10^{21}$)
48	Oriani [52]	SrCeO ₃ /D ₂	22	$Q \sim 0.7$ W	4.0×10^{10}	$V = 0.31 \text{ cm}^3$
49	Notoya [35"]	Ni/D,H/K	3.4×10^4	Q (0.9 W), t	2.4×10^{13}	(If half of T is in liquid)
50	Notoya [35-4]	Ni/D,H/K	same	NTD (Ca)	1.4×10^9	(Sintered Ni)
51	Yamada [54]	Pd/D ₂	185	n , NTD (C)	2.0×10^{12}	
52	Cuevas [55]	TiD _{1.5}	134	n (102 n/s)	5.4×10^{11}	
53	Niedra [56]	Ni/H/K	80	Q (4 W)	1.4×10^9	5 km x 0.5 mm ϕ
54	Ohmori [22"]	Au/H/K	200	Q , NTF (Fe)	$\sim 10^{11}$	(Au plate)
55	Li [57]	Pd/D ₂	185	Q	1.6×10^{12}	(Pd wire)
56	Qiao [57']	Pd/HZ	185	NTF (Zn)	3.8×10^{10}	(40%NTin ly)
57	Bressani [58"]	Ti/D ₂	≤ 10 ?	n (e)	$10 \sim 10^7$	(Ti shaving)
58	Miley [65]	Ni/H/Li	50	NTD (Fe, Cr.)	1.7×10^{12}	
59	Botta [58"]	Pd/D ₂	≤ 10 ?	He	7×10^{12}	(0.1 mm Pd sheet)
60	Coupland et al. [81]	Pd/H,D	4	$\Delta(\text{Li}/\text{Li})=60-90\%$ if $(7\text{Li}/6\text{Li})_0=12.5$	$3.5-4.1 \times 10^8$	Pd rod returned by F. and P. [1]
61	Passe11 [3-6]	Pd/H ₂	185(?)	$\Delta(\text{Li}/\text{Li})=100\%$	4.4×10^8	Pd wire [57-3]

NEUTRON CONDUCTION BAND AND NEUTRON VALENCE BAND [7,11-13]

Low-energy neutrons in crystal behaves as neutron Bloch waves with an energy spectra having a band structure (neutron conduction bands) [7] similar to the band structure of conduction electrons in solids familiar in solid state physics. The excited neutrons in nuclei on the lattice points of a solid (in lattice nuclei) can be mediated by hydro-

gen isotopes occluded in the solids to interact each other through the strong nuclear force (the super nuclear interaction) [11-13]. This super nuclear interaction results in a neutron bands below zero energy (neutron valence bands) made of excited neutron states in lattice nuclei.

LOCAL COHERENCE [8] OF NEUTRON BLOCH WAVES AT BOUNDARY

When the neutron Bloch waves with the same energy and different wave vectors in a band are reflected at a boundary, there appears the local coherence in the reflected waves and density of neutrons becomes very high at the boundary region [10]. In optimum cases, the density reaches the lower limit of that of neutron star matter [14,15]. As was shown by numerical simulation [15], there appears a lattice (a Coulomb lattice) of neutron-proton clusters (neutron drops) in a thin neutron gas just like a lattice of atoms in solids with parameters shown in Table 6.

TABLE 6. THEORETICAL AND EXTRAPOLATED TO $N_G = 1 \times 10^{30} \text{ cm}^{-3}$ VALUES OF THE LATTICE CONSTANT a OF COULOMB LATTICE AND THE PROTON-TO-NEUTRON RATIO \bar{x} IN THE NEUTRON DROPS (n - p CLUSTERS) AS FUNCTIONS OF n_G , WHERE n_G IS THE DENSITY OF THE NEUTRON GAS SURROUNDING THE NEUTRON DROPS IN THE COULOMB LATTICE.

For reference, a and \bar{x} for the lattice of Pd metal (composed of $^{110}_{46}\text{Pd}$) is added.

Density n_G (cm^{-3})	5×10^{37}	5×10^{36}	5×10^{35}	4×10^{34}	1×10^{30}	(Pd metal)
Estimated a (\AA)	4×10^{-4}	7×10^{-4}	8.7×10^{-3}	1.1×10^{-3}	2×10^{-3}	$a_{pd} = 2.5$
Estimated \bar{x}	0.28	0.45	0.53	$0.53 \sim$	0.7	$\bar{x}_{pd} = 0.72$

The lattice constant a and the proton-to-neutron ratio \bar{x} in the neutron drop (n - p cluster) of the Coulomb lattice are given as functions of n_G , the density of the neutron gas surrounding the nucleus. For reference, a and \bar{x} for the lattice of Pd metal (composed of $^{110}_{46}\text{Pd}$) is added. In this table, a value of n_G extrapolated to $1 \times 10^{30} \text{ cm}^{-3}$ is also included which is an attainable value in the boundary layers of CF materials [8,10].

NEUTRON DROPS [10] IN A THIN NEUTRON GAS

It was shown that neutron drops consisted of a large number of neutrons, and a few protons are formed when the density of neutrons is very high [10]. If we combine the conclusion of the Coulomb lattice formation by the simulation in neutron star matter and the conclusion of possible neutron drop formation in surface layers, we can deduce the following image of boundary layers in the transition-metal hydrides and deuterides, which is one of typical materials in which CFP is often observed.

The background thermal neutrons trapped in a sample of the transition-metal hydrides or deuterides are in a neutron conduction band. Their density becomes high at boundary region due to the local coherence but may be not so large and not enough to form a neutron drop yet. The neutrons in the band, however, can reacts with nuclei in the boundary region and the reactions are the trigger reactions explained in "Trigger Reactions." The nuclear products of the trigger reactions induce breeding reactions ("Breeding Reactions") resulting in multiplication of number of neutrons in the conduction band and also excitation of neutrons in lattice nuclei.

The latter effect makes possible formation of neutron valence bands in the material now being considering [13-15]. The density of neutrons in the neutron valence bands will be large enough to form neutron drops in the boundary region. The neutron drops thus formed are in a Coulomb lattice (neutron drop lattice) coexisting with the original crystal lattice of the transition metal. This is a new state of solids not noticed before and not observed until CFP was detected.

INTERACTION OF A NUCLEUS WITH A NEUTRON DROP [14,15]

The neutron drops thus formed interact with surrounding nuclei and can give nucleons to or exchange them with lattice nuclei (or nuclei of minor elements) in the boundary layer. This feature is formulated in "Neutron Drop-Nucleus Reactions" (above). Nuclear reactions investigated in nuclear physics in 20th century were mainly those that occur in free space except for rare cases of neutron-proton cluster formations in the neutron star matter [14,15]. The nuclear reactions in surface layers where coexist lattice nuclei, occluded hydrogen isotopes, and high density

neutrons should be distinguished from those occurring in free space and treated with cautions similar to those for the cluster formation in the neutron star matter [15].

Fundamental differences related with nuclear transmutations observed in CFP are possibilities of (1) nucleon exchange between lattice nuclei or minor nuclei and (2) energy exchange between surrounding neutron gas and/or neutron drops and nuclides in excited states. The former gives a possibility to generate new nuclides with largely different mass and proton numbers from lattice or minor nuclei in the system and the latter gives a possibility to stabilize excited states of nuclides without emission of γ -rays.

POSSIBILITY OF NT WITH LARGE CHANGES OF NUCLEON AND PROTON NUMBERS [16-25]

In our treatment of experimental data sets in CFP, we have used the TNCF model only using reactions (2), (3), (4), and (6) where occurs the absorption of a neutron by a nucleus to explain various events with successful results. The nuclear transmutations observed, however, have shown large changes of mass numbers up to several tens in the experiments showing NT_F [16-20] and recent experiment of NT_A [20-24], which needs the possibility to absorb large number of neutrons or sometimes clusters of neutrons and protons simultaneously. The formation of the neutron drops gives a natural explanation for these absorptions.

CONCLUSION

As we have seen in this paper, CFP is a phenomenon with many manifestations, including excess heat generation, three types of NT, production of light elements, T and ^4He , emission of neutrons, gammas and X-rays with various energies up to about 10 MeV, and decay-time shortening of radioactive nuclides [5,25]. It occurs in complex systems composed of transition-metal hydrides and deuterides and other materials on the surface at about room temperature in ambient radiation.

NATURE OF THE COLD FUSION PHENOMENON (CFP)

The cold fusion phenomenon occurs intermittently and sporadically with qualitative reproducibility in surface layers of a few micrometers thickness. As CFP occurs, the composition of CF materials inevitably changes due to nuclear transmutation and the structure of CF materials deteriorates. This may be the main cause of the intermittent occurrence and qualitative reproducibility of events in CFP.

POSSIBLE APPLICATIONS OF CFP

On the basis of these experimental facts and theoretical investigations, we can discuss possible applications of CFP for energy production and nuclear waste remediation. (1) Using appropriate transition metals, hydrogen isotopes to be occluded in them, and electrolytes in electrolytic systems, we can control nuclear reactions in solids, effectively producing excess heat and nuclear products. The same principle may be used for remediation of hazardous nuclear waste, transmuting it into non-radioactive nuclides. (2) One possible application of CFP at present is the use of excess energy. The energy liberated by nuclear reactions in the CF materials could be used for heating purposes. (3) Another anticipated application of CFP at present is in the transmutation of elements. The production of tritium is possible in the surface layers of CF materials by the reactions (3) and (4). Other promising applications are remediation of hazardous radioactive nuclides by NT and/or decay-time shortening into non-radioactive nuclides and utilization of heat energy from the system as an energy sources.

The NTs are a newly explored phase of CFP, and our knowledge about them is not complete. Further investigation of CFP will enable us to know more about the solid state-nuclear physics involved, an essential part of which should be neutron physics in solids.

ACKNOWLEDGMENT

The author would like to express his thanks to John Dash for valuable discussions during this work. This work is supported by a grant from the New York Community Trust.

REFERENCES

1. M. Fleischmann, S. Pons and M. Hawkins, "Electrochemically induced Nuclear Fusion of Deuterium," *J. Electroanal. Chem.*, v. 261, pp. 301-309, 1989.
2. S.E. Jones, E.P. Palmer, J.B. Czirr, D.L. Decker, G.L. Jensen, J.M. Thorne and S.E. Tayler, "Observation of Cold Nuclear Fusion in Condensed Matter," *Nature*, v. 338, pp. 737-740, 1989.

3. A.J. Leggett and G. Baym, "Exact Upper Bound on Barrier Penetration Probabilities in Many-Body Systems: Application to 'Cold Fusion,'" *Phys. Rev. Letters*, v. 63, pp. 191-194, 1989.
4. S. Ichimaru, "Nuclear Fusion in Dense Plasmas," *Rev. Mod. Phys.*, v. 65, pp. 255-299, 1993.
5. H. Kozima, *Discovery of the Cold Fusion Phenomenon - Evolution of the, Solid State - Nuclear Physics and the Energy Crisis in 21st Century*, Ohtake Shuppan KK., Tokyo, Japan, 1998. References of this book are posted on CFRL Website; <http://web.pdx.edu/pdx00210/Books/Discovery/disco.html>
6. H. Kozima, K. Kaki and M. Ohta, "Anomalous Phenomenon in Solids Described by the TNCF Model," *Fusion Technol.*, v. 33, pp. 52-62, 1998.
7. G. Baym, H.A. Bethe and C.J. Pethick, "Neutron Star Matter," *Nuclear Physics*, v.A175, pp. 225-271, 1971.
8. J.W. Negele and D. Vautherin, "Neutron Star Matter at Sub-nuclear Densities," *Nuclear Physics*, v. A207, pp. 298-320, 1973.
9. H. Kozima, "Neutron Band in Solids," *J. Phys. Soc. Japan*, v.67, pp. 3310-3311, 1998.
10. H. Kozima, K. Arai, M. Fujii, H. Kudoh, K. Yoshimoto and K. Kaki, "Nuclear Reactions in Surface Layers of Deuterium-Loaded Solids," *Fusion Technol.*, v. 36, pp. 337-345, 1999.
11. H. Kozima, M. Ohta, M. Fujii, K. Arai and H. Kudoh, "Possible Explanation of 4He Production in a Pd/D2 System by the TNCF Model," *Fusion Science and Technology*, v. 40, pp. 86-90, 2001.
12. H. Kozima, "Neutron Drop: Condensation of Neutrons in Metal Hydrides and Deuterides," *Fusion Technol.*, v. 37, pp. 253-258, 2000.
13. H. Kozima, "Excited States of Nucleons in a Nucleus and Cold Fusion Phenomenon in Transition-Metal Hydrides and Deuterides," *Proc. ICCF9* (to be published); *Abstracts of ICCF9*, pp. 56-57, 2002.
14. H. Kozima, J. Warner and G. Goddard, "Cold Fusion Phenomenon and Atomic Processes in Transitionmetal Hydrides and Deuterides," *J. New Energy*, v. 6-2, pp. 126-141, 2001.
15. H. Kozima, "Anomalous Nuclear Reactions and Atomic Processes in Transition-Metal Hydrides and Deuterides" *J. New Energy*, v. 6-3 (2002). (to be published)
16. J.O.M. Bockris and Z. Minevski, "Two Zones of "Impurities" Observed after Prolonged Electrolysis of Deuterium on Palladium," *Infinite Energy*, #5 & 6, pp. 67-75, 1995-96.
17. G.H. Miley, G. Narne, M.J. Williams, J.A. Patterson, J. Nix, D. Cravens and H. Hora, "Quantitative Observation of Transmutation Products Occurring in Thin-Film Coated Microspheres during Electrolysis," *Progress in New Hydrogen Energy (Proc. ICCF6)*, pp. 629-644, 1996.
18. T. Ohmori, M. Enyo, T. Mizuno, Y. Nodasaka and H. Minagawa, "Transmutation in the Electrolysis of Light Water - Excess Energy and Iron Production in a Gold Electrode," *Fusion Technol.*, v. 31, pp. 210-218, 1997.
19. T. Mizuno, T. Akimoto, T. Ohmori and M. Enyo, "Confirmation of the Changes of Isotopic Distribution for the Elements on Palladium Cathode after Strong Electrolysis in D2O Solution," *Int. J. Soc. of Materials Engin. for Resources*, v. 6-1, pp. 45-59, 1998.
20. H. Yamada, S. Narita, Y. Fujii, T. Sato, S. Sasaki and T. Omori, "Production of Ba and Several Anomalous Elements in Pd under Light Water Electrolysis" *Proc. ICCF9* (to be published); *Abstracts of ICCF9*, p. 123 (2002). (Pd → Ba, Pb)
21. S. Miguet and J. Dash, "Microanalysis of Palladium after Electrolysis in Heavy Water," *Proceedings of 1st Low Energy Nuclear Reactions Conference*, College Station, Texas, pp. 23-27, 1995. (Pd → Cd).
22. R. Kopecek and J. Dash, "Excess Heat and Unexpected Elements from Electrolysis of Heavy Water with Titanium Cathodes," *Proceedings of 2nd Low Energy Nuclear Reactions Conference*, College Station, TX, pp. 46-53, 1996. (Ti → Cr).
23. J. Warner and J. Dash, "Heat Production during the Electrolysis of D2O with Titanium Cathodes," *Conference Proceedings 70 (Proceedings of 8th International Conference on Cold Fusion, Leri, Italy)*, pp. 161-167, 2000. (Ti → Cr).
24. Y. Iwamura, M. Sakano and T. Itoh, "Elemental analysis of Pd Complexes: Effects of D2 Gas Permeation," *JPN. J. Appl. Phys.*, v. 41, pp. 4642-4650, 2002. (Cs → Pr, Sr → Mo)
25. J. Dash, I. Savvatimova, G. Goddard, S. Frantz, E. Weis and H. Kozima, "Effects of Hydrogen Isotope on Radioactivity of Uranium," *Proc. ICENES2002* (to be published). (928U → 904Th)